Publishing House
AKAPIT

COMPUTER METHODS IN MATERIALS SCIENCE
Informatyka w Technologii Materiałów

Vol. 15, 2015, No. 1

APPLICATION OF THE FULLY AUTOMATIC *HP*-ADAPTIVE FEM TO ELASTIC-PLASTIC PROBLEMS

MARTA OLEKSY*, WITOLD CECOT

Institute for Computational Civil Engineering,Cracow University of Technology,
ul. Warszawska 24, 31-155 Kraków, Poland
**Corresponding author: moleksy@L5.pk.edu.pl*

Abstract

The *hp*-adaptive mesh refinement is a technique that for linear problems proved to deliver a fast, predicted by theory, exponential convergence. We have applied this approach to elastic-plastic problems modeled by associative constitutive law with the Mises yield surface. A modification of the automatic refinements and various types of mesh adaptation were tested. Exponential convergence was observed when the FEM mesh complied with the yielding zone. In general the original automatic *hp*-mesh **r**efinements led to the fastest convergence even though it was only algebraic, what is theoretically justified for elastic-plastic problems.

Key words: fully automatic *hp*-adaptivity; elastic-plastic problem; exponential convergence

1. INTRODUCTION

Since the eighties of the 20th century both h and p adaptive mesh refinements were used by many researchers to improve convergence of the FEM solutions for inelastic problems. Cheng (1988) as well as Zienkiewicz and coworkers (Zienkiewicz et al., 1990) developed this approach to metal forming processes, Peric, Dutko and Owen (Peric et al., 1996; Peric et al. 1998) presented adaptive FEM solutions for large strain plasticity, Cramer et al. (1999) applied partitioning of elements to associative and non-associative plasticity. Ladeveze and Moes (1999) proposed a posteriori error estimation, to control time-dependent nonlinear finite element analysis. They used the error and the three indicators in an adaptive strategy (to adapt the mesh, the time and to limit the number of iterations of the global iterative algorithm). Johnson and Hansbo (Johnson et al., 1992) have developed adaptive strategy, based on residual error estimator, for small strain elastoplasticity using the Hencky model. Adaptive mesh refinement procedure, based on a-posteriori estimate, that takes into account the local directional interpolation error and a recovering technique to compute second derivatives of the finite element solution was proposed by Borges and coworkers (Borges et al., 2001) for limit analysis. This approach is able to capture discontinuities arising from localized plastic deformations during plastic collapse. The p-adaptive FEM was reported to be efficient approximation to physically nonlinear problems by Düster and Rank (2002) since elastic-plastic solution may be highly regular in interior of both elastic and plastic subdomains. The rp-adaptive approach was used by Nübel and coworkers (Nübel et al., 2007) to adjust finite element mesh to elastic-plastic border in order to take into account the loss of regularity and consequently observed exponential convergence rate for deformation theory of plasticity.

In this work we examined convergence of the fully automatic hp strategy, developed by Demkowicz and coworkers (Demkowicz, 2006; Dem-

 ISSN 1641-8581

kowicz et al., 2007). This method leads to the exponential convergence for linear problems (Demkowicz et al., 2002; Gui & Babuška, 1986). In order to obtain an efficient method for elastic-plastic computational homogenization of metal matrix composites (Serafin & Cecot, 2010). We have applied the self adaptive *hp*-FEM to inelastic problems. Even though the elastic-plastic solutions are, in general, not analytic almost everywhere (Szabo et al., 2004) and consequently exponential convergence for *hp*-FEM is not guaranteed, one may still expect a faster convergence of hp than exclusively h or p mesh refinements.

2. FORMULATION OF THE PROBLEM

We consider here quasi-static elastic-plastic processes under small displacements and strains for polycrystalline materials with linear, kinematic hardening. Such processes may be modeled by associative plasticity with certain yield function (denoted by Φ), resulting in the following initial boundary value problem defined in an open bounded domain $\omega_e \cup \omega_p = \Omega \subset \boldsymbol{R}^n$, n = 1, 2 or 3 and pseudo-time interval [0, T], where ω_e and ω_p are elastic and plastic subdomains (zones):
find sufficiently regular fields of displacements u(x; t), strains ε(x; t), inelastic strains $\varepsilon^p(x;t)$, plastic multiplier γ(x; t) (γ(x; t) = 0 in ω_e) and stresses σ(x; t) such that:

$$\begin{cases} div\dot{\sigma} = 0 & \forall x \in \omega_e or \omega_p, \forall \tau \in [0,T] \\ \dot{\varepsilon} = \frac{1}{2}\left[\nabla \dot{u} + (\nabla \dot{u})^T\right] & \forall x \in \omega_e or \omega_p, \forall \tau \in [0,T] \\ \dot{\sigma} = C\left(\dot{\varepsilon} - \dot{\varepsilon}^p\right) & \forall x \in \omega_e or \omega_p, \forall \tau \in [0,T] \\ \dot{\varepsilon}^p = \gamma \frac{\partial \Phi}{\partial \sigma} & \forall x \in \omega_e or \omega_p, \forall \tau \in [0,T] \\ \gamma \geq 0, \Phi \leq 0, \gamma\Phi = 0 & \forall x \in \omega_e or \omega_p, \forall \tau \in [0,T] \\ \dot{u} = \hat{\dot{u}} & \forall x \in \omega_e or \omega_p, \forall \tau \in [0,T] \\ \dot{\sigma} n = \hat{\dot{t}} & \forall x \in \omega_e or \omega_p, \forall \tau \in [0,T] \\ \varepsilon^p = \varepsilon^p_0, u = u_0 & \forall x \in \omega_e or \omega_p, \forall \tau \in [0,T] \end{cases} \tag{1}$$

where, as usual, the Lipschitz boundary $\partial\Omega = \overline{\partial\Omega_D} \cup \overline{\partial\Omega_N}$ and $\partial\Omega = \overline{\partial\Omega_D} \cap \overline{\partial\Omega_N} = \emptyset$. For $n > 1$ the measure of Dirichlet boundary is greater than zero (meas $\partial\Omega_D > 0$). We also assume that the initial conditions are compatible with both loading and plastic strains. Furthermore, continuity of displacement and stress vectors holds on the elastic-plastic interface at every time instant. Integration in time of problem (1) is usually performed by the backward Euler scheme with return mapping corrector (see e.g. Simo & Hughes, 1998). After converting the rate formulation into the incremental form, the total load history is represented by a sequence of sub-loads. For each sub-load the solution increment is evaluated iteratively by requiring at each Gauss integration point fulfillment of the yield condition and overall momentum equations at the end of each load increment. The well known algorithm makes use of the decomposition of the stress increment into two parts: the elastic trial component (σ^{trial}) and the plastic corrector component ($\Delta\sigma = -C\Delta\varepsilon^p$) evaluated by the return mapping method (Simo & Taylor, 1986) (radial return algorithm for the Mises yield function). The trial part is computed, for fixed plastic strain increment $C\Delta\varepsilon^p$, by the momentum equation $(1)_1$ combined with equations $(1)_{2,3}$. Then the plastic flow rule and the yield condition constitute, in the case of constant hardening, the following nonlinear system of equations that is used to define increments of the corrector parts of stress (Δσ) and the plastic multiplier (Δγ)

$$\begin{cases} C^{-1}\Delta\sigma + \Delta\gamma \frac{\partial \Phi}{\partial \sigma} = 0 \\ \Phi\left(\sigma^{trial} + \Delta\sigma\right) = 0 \end{cases} \tag{2}$$

The system of equations (2) is, in general, solved by the Newton-Raphson method. Usually, in order to assure quadratic convergence of the iterative process, the so-called algorithmic tangent modulus is suggested instead of tangent one.

3. AUTOMATIC MESH ADAPTATION

The automatic mesh adaptation proposed in (Demkowicz et al., 2002) was successfully used for various linear problems. Its key idea is an appropriate strategy of anisotropic *h*, *p* or *hp* mesh refinement. It is based on the interpolation error estimate, which is a good upper bound of the best approximation error that in turn, for coercive problems by the Cea's lemma, is the upper bound for the actual approximation error. The aforementioned interpolation error is estimated by making use of a fine mesh solution ($u_{h/2,p+1}$, denoted here for the sake of brevity by u) that serves as a substitute for the exact solution. Such an "exact" solution is interpolated locally on possible new *hp*-refined meshes. The difference between u and its interpolant approximates the interpolation error and the optimal anisotropic mesh refinement is that one for which the reduction of the interpolation error per number of additional degrees of freedom is maximal. It means, that for the coarse mesh the optimal (h, p or hp) refinement is determined by maximizing the following expression

$$r = \frac{\left|u - \Pi_{hp} u\right|^2_{H^1} - \left|u - \Pi_{hp_{opt}} u\right|^2_{H^1}}{N_0 - N_c} \rightarrow \max \quad (3)$$

with additional assumption, that the mesh is oneirregular, where hp, h_{popt} denote H^1 projection-based interpolants on the current and optimal meshes, respectively; N_0, N_c are the numbers of degrees of freedom in optimal and current meshes. The maximization is performed by search over a suitable subset of all possible hp refinements. Thus, the algorithm of adaptation approach starts with the solution of the problem on the current (coarse) mesh (u_{hp}). Then, the refinement in both h and p is performed and the optimal mesh is selected by maximization of the function r defined by equation (3). For large problems computation of the fine mesh solution may be time consuming. However, only partially convergent solution obtained by e.g. a fast two-grid solver may be used to guide the optimal hp-refinement. For elastic-plastic problems accuracy of integration in semi-time τ depends primarily on accuracy of stress approximation in space since both plastic multiplier and plastic strain rate are determined by stress rate (equation $(1)_4$, $(1)_5$). Incremental application of loading reduces number of iterations and prevents numerical solution from coming to far away from the true one. Since solution $u_{h/2,p+1}$ uses significantly greater number of degrees of freedom therefore, the error of plastic strain approximation is also taken into account by the error estimate used in the automatic hp-adaptivity algorithm. Consequently, one may expect a fast exponential convergence also for elastic-plastic problems. In order to obtain appropriate stress approximation accuracy, inelastic deformations should be accounted for in a special way in a-posteriori error estimates (Barthold et al., 1998; Gallimard et al., 1996; Nübel et al., 2007; Peric et al., 1994). Therefore, we have studied performance of the original and modified automatic hp-mesh refinement for elasticplastic problems. The objective of the modification was an additional h-refinement of the mesh along the elastic-plastic interface, which is a place of lower solution regularity.

4. NUMERICAL TESTS – 1D EXAMPLES

The first (1D) numerical tests were performed for a bar subject to axial body force.

$$q(x) = -\sin(2\pi x)\, 2\sigma_0 x \quad (4)$$

For the considered example the following material properties were assumed: Young modulus E = 200 GPa, Poisson ratio $\nu = 0.3$, yield stress limit σ_0 = 200 MPa and hardening parameter $H = 0.2E$. The second derivative of the exact solution is not continuous at the elastic-plastic interface thet for this data is located at points $x = 0.25$, $x = 0.75$. First, p-stability for presented example was verified and the results presented in figure 1 indicate, that p-enrichment is reasonable for our problem since it reduces the error. The main objective of the tests was verification whether the fully automatic hp-refinements should be complemented with additional h-refinements (or p-enrichment) in vicinity of the elastic-plastic zone. The asymptotic behavior of the solution below the error level of 10^{-6} is a result of the tolerance assumed for meeting the yield condition in the radial return algorithm.Therefore, in all the examples considered in this paper the analysis was performed at most as long as this error level was reached.

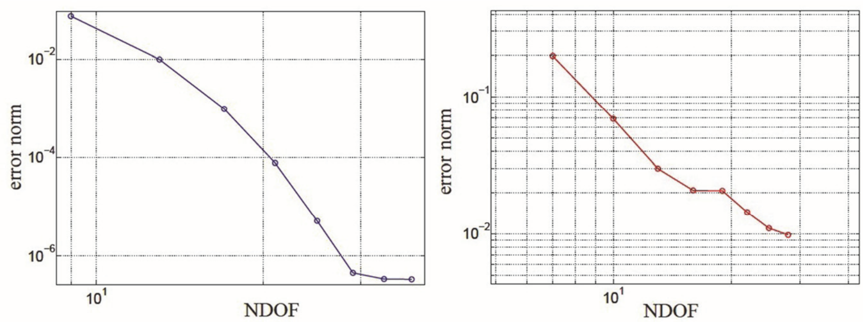

Fig. 1. First 1D example. p-stability for meshes that initially did or did not comply with elastic-plastic zones.

Since the rate of convergence is much better for the meshes that initially comply with the elastic-plastic interface, the numerical analysis with two initial meshes was performed in order to examine the adaptation process for inelastic problems. In the first case the initial finite element mesh complied with a-priori known elastic and plastic zones, while in the second case initial mesh was independent of yielding. In the second case we have observed, that after few automatic adaptation steps the mesh accommodated to elastic-plastic interfaces at points x = 0.25 and x = 0.75 (first 1D example), as may be observed in figure 2. Convergences of the error norm for various refinement strategies are compared in figures 3, 4. One may observe that in the first case, i.e. with initially detected elastic-plastic interface, the results are better.

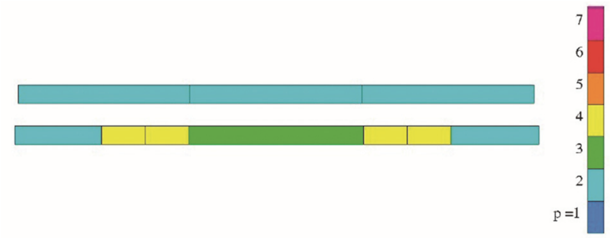

Fig. 2. First 1D example. Initial and hp-refined meshes (colors indicate order of approximation).

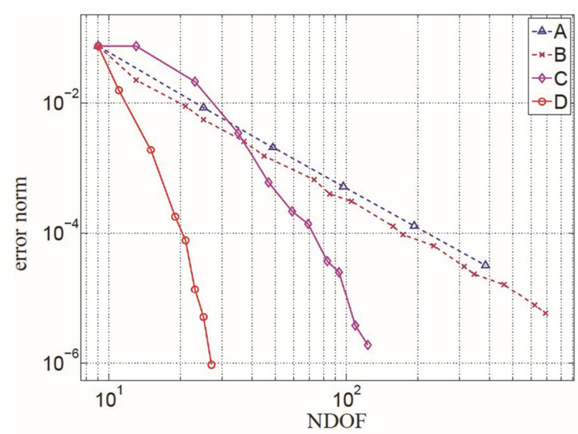

Fig. 3. First 1D example. Convergence test for the mesh that initially complied with elastic-plastic zone. A – uniform refinement, B – h-adaptation, C – automatic hp-adaptation with additional h-refinements of neighboring elements, D – automatic hp-adaptation.

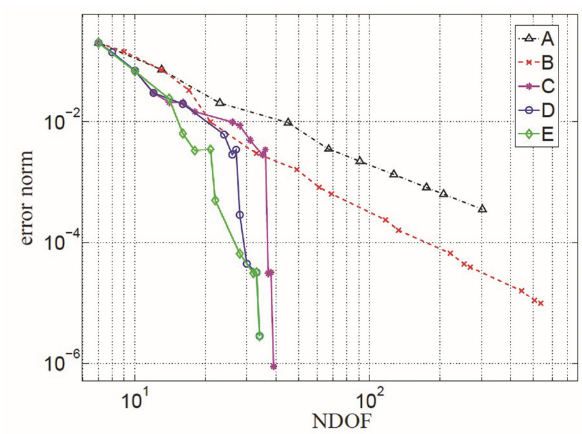

Fig. 4. First 1D example. Convergence test for the mesh that did not comply with elastic-plastic zone. A – uniform refinement, B – h-adaptation, C – automatic hp- adaptation with additional p-enrichment, D – automatic hp-adaptation, E – automatic hp-adaptation with additional h-refinements.

To make an example more realistic we assumed the elastic-plastic interfaces at points x = 0.23456789 and x = 0.703703670 (second 1D example). In this case only meshes that did not comply with elastic plastic interface were used. The corresponding plastic strain distribution and the resulting mesh refinements are presented in figure 5. In this example the p-stability was also observed (figure 6) and convergence of error norm for different refinements is presented in figure 7.

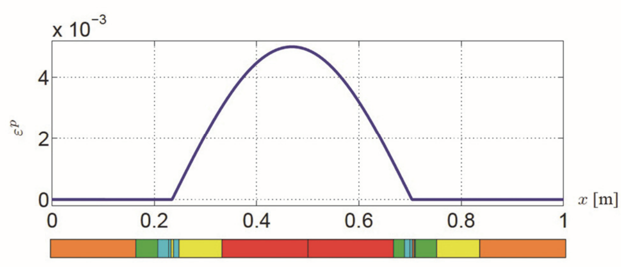

Fig. 5. Second 1D example. Plastic strain and mesh after few steps of hp-adaptation.

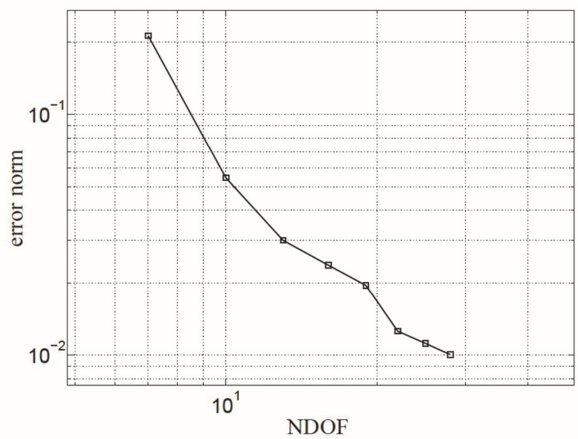

Fig. 6. Second 1D example. p-stability.

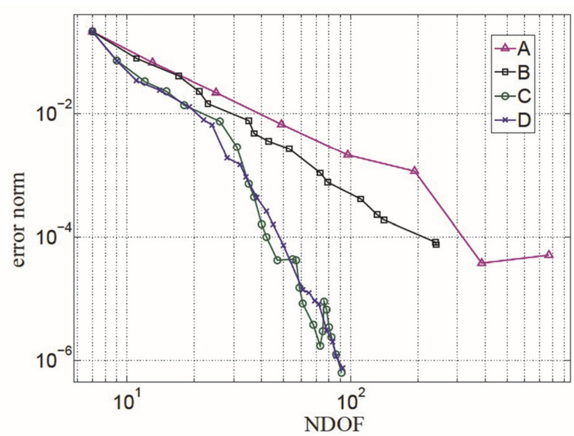

Fig. 7. Second 1D example. Convergence test for mesh that did not account for elastic-plastic zone. A – uniform refinement, B – h-adaptation, C – automatic hp-adaptation with additional h-refinements, D – automatic hp-adaptation.

In the 1D examples additional h-refinements maybe profitable for convergence rate. However, since 1D problems may exhibit super convergence properties the further tests were performed for 2D examples.

5. NUMERICAL TESTS – 2D EXAMPLES

The following 2D examples were examined:
1. thick-walled cylinder
2. L-shaped domain
3. perforated plate
4. non-perforated plate 1
5. non-perforated plate 2

All these examples may be formulated in the following weak form: *find field of displacements* $\boldsymbol{u}(x; t) \in \boldsymbol{V}_0 + \hat{\boldsymbol{u}}$ *, such that for every* $t \in [0; T]$

$$\int_\Omega \varepsilon(\boldsymbol{v}) : C\dot{\varepsilon}(\dot{\boldsymbol{u}}) d\Omega = \int_\Omega C\dot{\varepsilon}^p d\Omega + \int_{\Gamma_N} \hat{\boldsymbol{t}} \boldsymbol{v} ds \forall v \in \boldsymbol{V}_0 \tag{5}$$

where $\boldsymbol{V}_0 = \{\boldsymbol{v} \in [H^1(\Omega)]^n, \boldsymbol{v} = 0 \text{ on } \partial\Omega_D\}$, $\partial\Omega_D$ and $\partial\Omega_N$ are the Dirichlet and Neumann parts of the boundary, $\partial\Omega_D \cup \partial\Omega_N = \partial\Omega$ and $\partial\Omega_D \cap \partial\Omega_N = \emptyset$. $\hat{\boldsymbol{t}}, \hat{\boldsymbol{u}}$ are known tractions and displacements along the Neumann and Dirichlet parts of the boundary, C stands for elastic tensor of material parameters. For each example the following data were assumed: Young modulus E = 200 GPa, Poisson ratio $\nu = 0.3$, yield limit σ_0 = 200 MPa, hardening parameter $H = 0.1E$. In 2D examples additional h-refinements for elements with both elastic and plastic zones were performed in order to fit better to the zones. These additional refinements were performed by considering four closest to vertices Gauss integration points. If only at two of those points located near one common edge (marked by the red color in figure 8) material yields, then the element is partitioned in the direction perpendicular to that common edge. Otherwise, if yielding is observed at some, but not all of Gauss points, the uniform h-refinement is performed.

5.1. Thick-walled cylinder

We assumed plane strain state for a quarter of a thick-walled cylinder with radii 1 m and 2 m. It was loaded by internal pressure p = 120 MPa, that resulted in yielding at points in distance smaller then ~1.226 m from the center. The finite element mesh initially did not comply with the elastic-plastic interface and consisted of 8 second order elements (2 in the radial and 4 in the hoop directions). Automatic hp-adaptation was performed in the standard way (FE mesh after few steps of adaptations is shown in figure 9) and it was compared with some other possible refinements (figure 12). We assumed the same as in figure 2 meaning of colors in all figures that present FEM meshes. In one of them hp-adaptation was augmented with additional h-refinements (figure 10). The proposed modification, based on additional refinements, resulted in better convergence and higher order approximation in the elastic zone. For comparison, finite element mesh, which complies with elastic-plastic interface was assumed (figure 11) and automatically refined. As one may expect in such a situation the best convergence was observed.

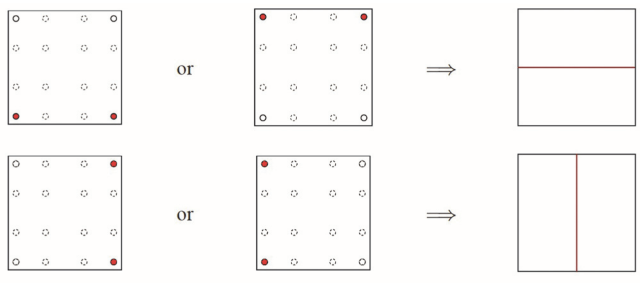

Fig. 8. *Cases of additional anisotropic element refinement.*

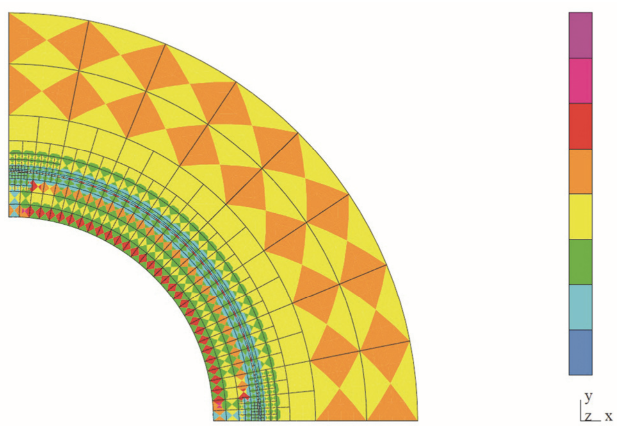

Fig. 9. *Cylinder test. Mesh after 20 steps of hp-refinements (colors indicate order of approximation).*

5.2. L-shaped domain

Another classical test, i.e. L-shaped domain with singular derivatives of solution at the reentrant corner was also considered. We assumed plane strain state, fixed boundary on the right-hand side and loading presented in figure 13. The finite element meshes obtained by various adaptation strategies are shown in figure 14. The elastic-plastic interface was successfully modeled by additional h-refinements of the partially yielded elements. In this example such a modification of adaptation process did not improve error convergence and the best one was observed for the original algorithm (figure 15). However, the number of necessary adaptation steps, that guarantees results with assumed accuracy, was reduced whenever the additional h-refinements were used.

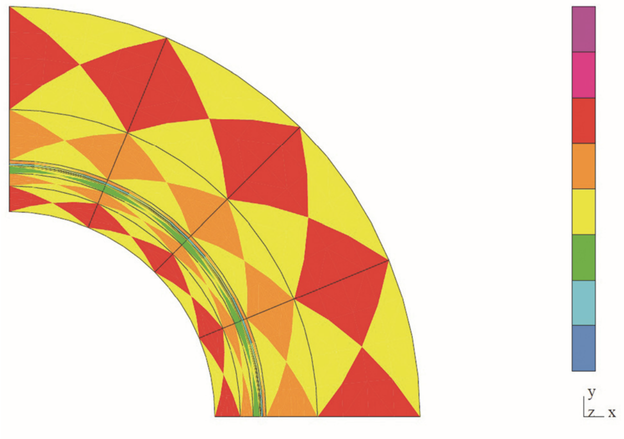

Fig. 10. Cylinder test. Mesh after 14 steps of modified hp-refinements.

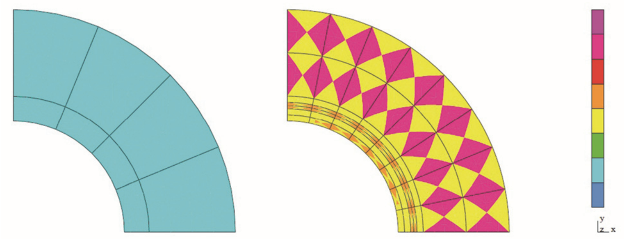

Fig. 11. Cylinder test. Initial mesh and after 13 steps of hp-refinements

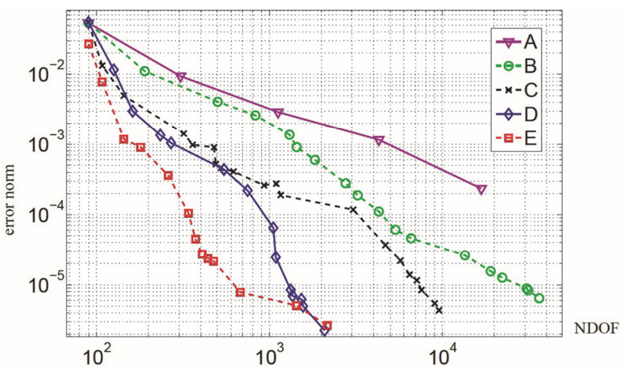

Fig. 12. Cylinder test. Convergence of error norm. A – uniform refinement, B – h-adaptation, C – original automatic hp-adaptation, D – automatic hp-adaptation with additional h-refinements of elements with both elastic and plastic zones, E – automatic hp-adaptation for mesh, which initially complies with known elastic-plastic interface.

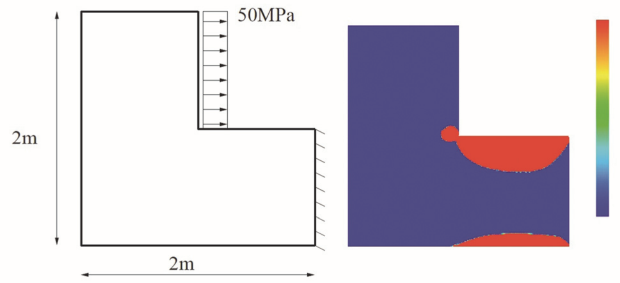

Fig. 13. L-shaped domain. Boundary conditions. Elastic (the blue color) and plastic (the orange color) subdo- mains.

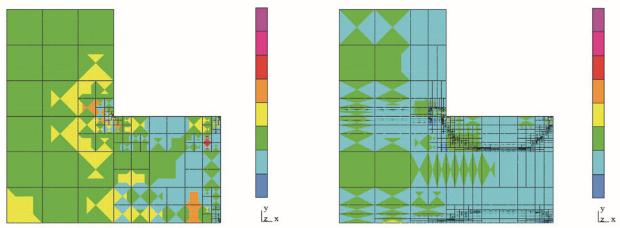

Fig. 14. L-shaped domain. Meshes after 18 steps of hp-refinements and 14 modified hp-refinements.

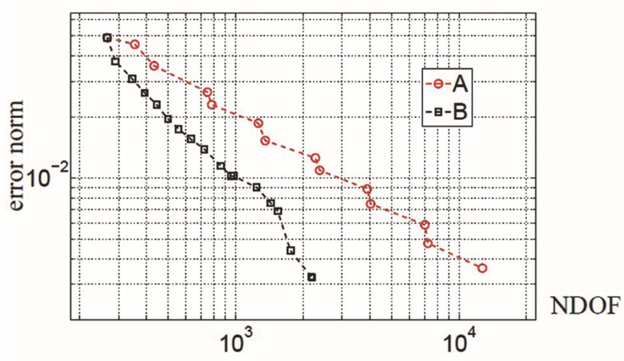

Fig. 15. L-shaped domain. Convergence history (A – automatic hp-adaptation with additional h-refinements, B – original automatic hp-adaptation.)

5.3. Perforated plate

A quarter of a perforated plate in plane strain state with constant loading was analyzed as a next test. Assumed boundary conditions and loading are shown in figure 16. The next figures present meshes obtained by fully automatic refinement of *hp* and *h*-type (figure 17), as well as after additional *h*-refinements along elastic-plastic interface (figure 18). This time, as it can be observed in the plot of convergence history, the rate of convergence was not improved by additional enforcement of mesh accommodation to plastic zone, but the number of refinement steps was two times smaller.

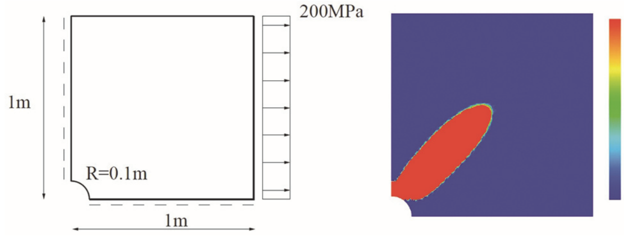

Fig. 16. *Perforated plate. Boundary conditions. Elastic and plastic zones.*

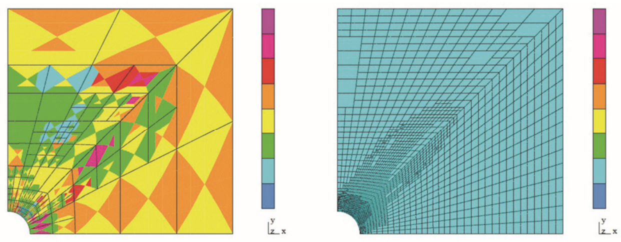

Fig. 17. *Perforated plate. Meshes after 20 steps of hp-refinements and 16 exclusively h-refinements.*

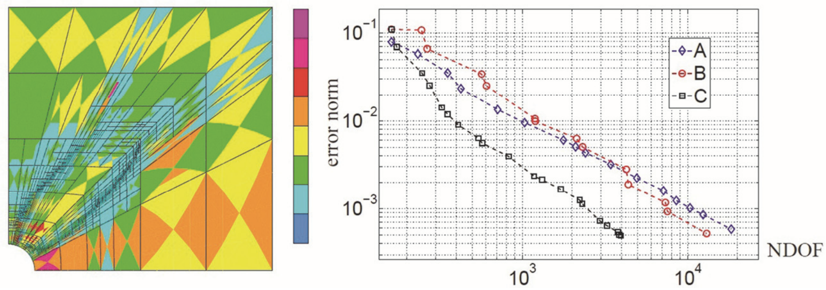

Fig. 18. *Perforated plate. Mesh after 15 steps of modified hp-refinements and convergence history (A – adaptive h-refinement, B – automatic hp-adaptation with additional h-refinements, C – original automatic hp- adaptation).*

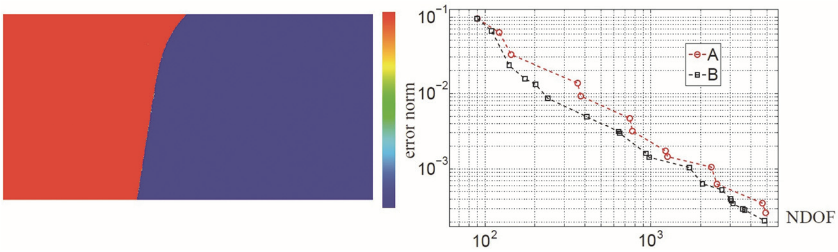

Fig. 19. *Non-perforated plate 1. Equivalent and plastic zones. Convergence history (A – automatic hp-adaptation with additional h-refinements, B – original automatic hp-adaptation).*

5.4. Non-perforated plate 1

In this example elastic-plastic deformations resulted in a rectangular plate ($1m \times 2m$) from body forces assumed in the form:

$$f_x = \frac{-\sigma_0 \pi}{2} \sin\left(\frac{\pi x}{4}\right), f_y = \frac{-\sigma_0 \pi}{2} \cos\left(\frac{\pi y}{4}\right) \quad (6)$$

Such a loading was assumed in order to be able to generate various shapes of elastic-plastic interfaces. Symmetry along left and bottom edges, as well as traction-free boundary conditions on the remain- ing edges were assumed. The elastic and plastic zones convergence history, as well as the meshes obtained by various strategies are shown in figures 19, 20. Convergence history for the modified automatic mesh adaptation was slightly worse than for the original version. This time the number of necessary refinements was also reduced.

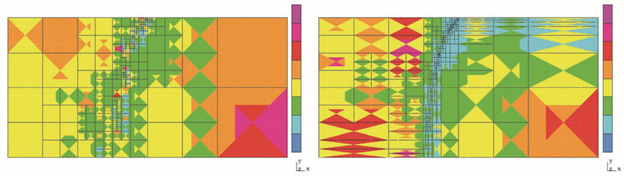

Fig. 20. *Non-perforated plate 1. Mesh after 15 steps of hp-refinements and 12 steps of modified hp-refinements.*

5.5. Non-perforated plate 2

The plate, fixed on the left edge and loaded on the right-hand side, was the next test (figure 21). A plane strain state was assumed. The results are presented in figures 22, 23. We may observe, for this elastic-plastic problem with singularity of solution, that the convergence rate for the original automatic *hp*-adaptation is much better than for the version with additional *h*-refinements.

6. SOLUTION TRANSFER

In all the examples described in this paper loading was applied in one step. Therefore, there was no need for solution transfer. However, if more steps were used the solution transfer would have to be done and it might be performed comparatively easily since the mesh is refined by subdivision of the elements (Wunderlich et al., 1998). Therefore, each new element is a part of only one old element. After a mesh refinement or unrefinement the time integration is performed on a new set of the Gauss points and accuracy of the space approximation changes. We propose the strategy that assumes a reanalysis of the actual load increment. Whenever the mesh is refined at the end of the load increment the second run over this increment should serve the purpose of solving the problem with specified accuracy in order to avoid the situation when large error in one time instant, that results from too coarse space discretization, influences the accuracy in the later time instances.

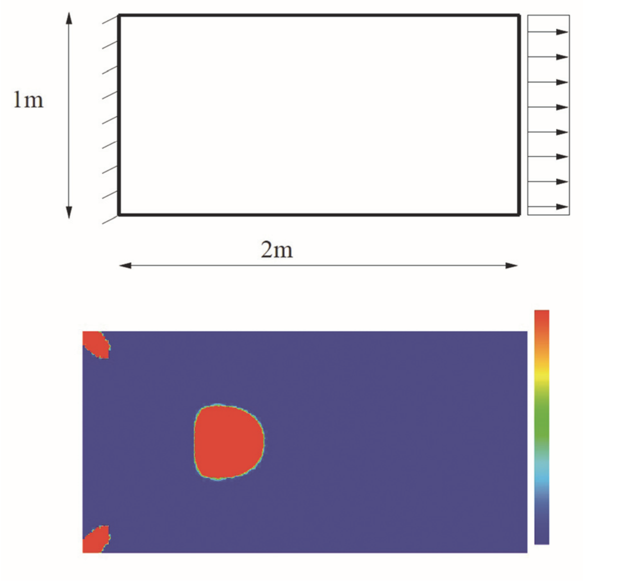

Fig. 21. Non-perforated plate 2. Boundary conditions. Elastic and plastic subdomains.

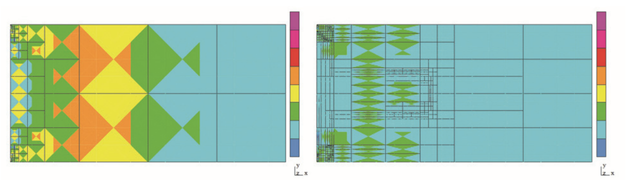

Fig. 22. Non-perforated plate 2. Mesh after 15 steps of hp-refinements and 14 steps of modified hp-refinements.

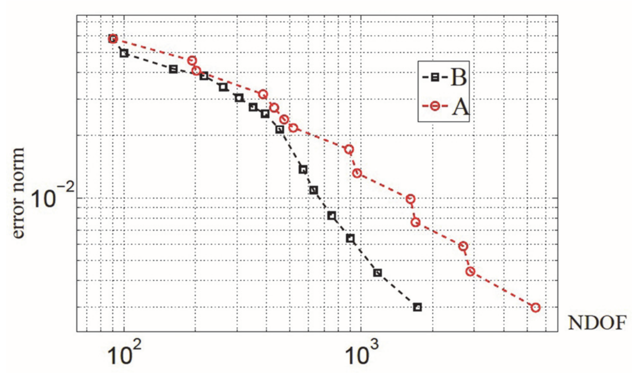

Fig. 23. Non-perforated plate 2. Convergence his- tory (A – automatic hp-adaptation with additional h-refinements, B – original automatic hp-adaptation).

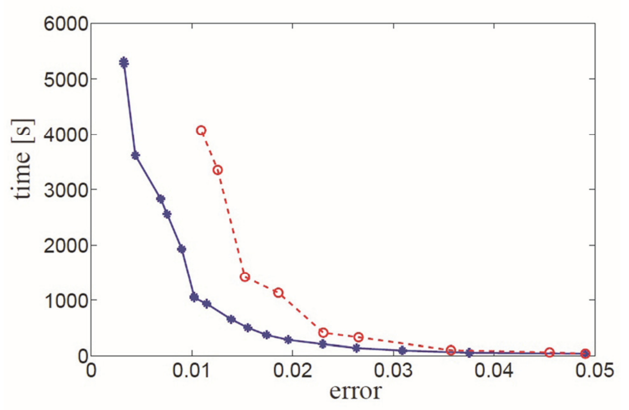

Fig. 24. L-shaped domain. Comparison of computation time (the continuous blue line – original hp-adaptation process, the dashed red line – original hp-adaptation process modified by additional h-refinements).

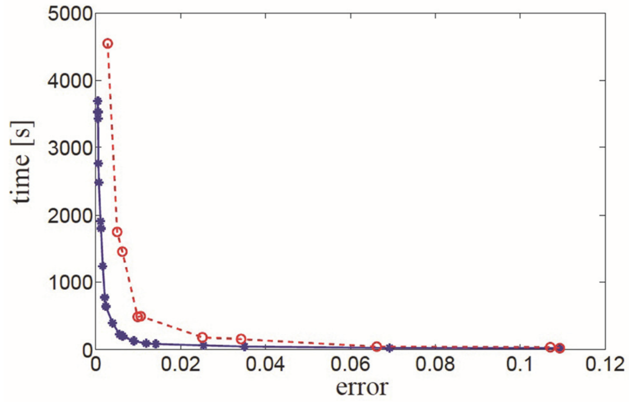

Fig. 25. Perforated plate. Comparison of computation time (the continuous blue line – original hp-adaptation process, the dashed red line – original hp-adaptation process modified by additional h-refinements).

7. CONCLUDING REMARKS

The fully automatic (self automatic) *hp*-adaptive mesh refinement strategy was applied to analysis of elastic-plastic problems. Since the solution is less regular at the elastic-plastic interface (Nübel et al., 2007) the finite element meshes should comply with elastic and plastic zones. However, the elastic and plastic zones are not known a-priori thus appropriate adaptive mesh refinements are the way to construct meshes that at least approximately correspond to the shapes of the zones. Generally, the self adaptive mesh refinement technique generates the aforementioned meshes and for the considered physically nonlinear problems and various types of mesh adaptation strategies delivers the fastest convergence of the error. We tested additional *h*-refinements and *p*-enrichments along the elastic-plastic interface, as well as exclusively *h*-adaptive or *p*-adaptive mesh refinements. Only in the case of cylinder additional *h*-refinements resulted in a speed up of the convergence. Presumably the reason for significant improvement only in this case was the shape of elastic-plastic interface, which could be relatively easily captured in the cylinder. In the other examples even anisotropic additional *h*-refinements did not result in meshes that exactly complied with elastic-plastic zones. Therefore, neither convergence rate nor time of computation (figures 24, 25) were improved and the original *hp*-FEM delivered the fastest theoretically justified algebraic convergence. In the future the fully automatic *hp* mesh refinements will be supplemented with the *r*-adaptation, since it was successfully used for *p*-refinements (Nübel et al., 2007). Also the algorithm of searching for the optimal new *hp* meshes should undergo further testing. Currently, for the sake of efficiency, only certain selected from all possible refinements are considered. Such a strategy works correctly for linear problems but its validation for elasto-plasticity is intended.

ACKNOWLEDGMENT

This research was supported by the National Science Center under grant 2011/01/B/ST6/07312.

REFERENCES

Barthold, F., Schmidt, M., Stein, E., 1998, Error Indicators and Mesh Refinements for Finite Element Computations of Elastoplastic Deformations, *Comput Mech*, 22, 225-238.

Borges, L., Zouain, N., Costa, C., Feij, R., 2001, An Adaptive Approach to Limit Analysis, *Int J Solids Struct*, 38, 1707-1720.

Cheng, J. H., 1988, Automatic Adaptive Remeshing for Finite Element Simulation of forming Processes, *Int J Numer Meth Eng*, 26, 1-18.

Cramer, H., Findeiss, R., Steinl, G., Wunderlich, W., 1999, An Approach to the Adaptive Finite Element Analysis in Associated and Non-associated Plasticity Considering Localization Phenomena, *Comput Method Appl M*, 176, 187-202.

Demkowicz, L., 2006, *Computing with hp-Adaptive Finite Elements. Vol. 1. One and Two Dimensional Elliptic and Maxwell Problems*, Chapman & Hall CRC.

Demkowicz, L., Kurtz, J., Pardo, D., Paszynski, M., Rachowicz, W., Zdunek, A., 2007, *Computing with hp Finite Elements. Vol 2. Frontiers: Three-Dimensional Elliptic and Maxwell Problems with Applications*, Chapman & Hall CRC.

Demkowicz, L., Rachowicz, W., Devloo, Ph., 2002, A Fully Automatic *hp*-Adaptivity, *J Sci Comput*, 17, 127-155.

Düster, A., Rank, E., 2002, A p-Version Finite Element Approach for Two- and Three-Dimensional Problems of the J2 Flow Theory with Non-Linear Isotropic Hardening, *Int J Numer Meth Eng*, 53, 49-63.

Gallimard, L., Ladeveze, P., Pelle, J., 1996, Error Estimation and Adaptivity in Elastoplasticity, *Int J Numer Meth Eng*, 39, 189-217.

Gui, W., Babuška, I., 1986, The *h*, *p* and *hp* Versions of the Finite Element Method in One Dimension. Parts 1,2,3, *Numer Math*, 49, 577-683.

Johnson, C., Ladeveze, P., Hansbo, P., 1992, Adaptive Finite Element Methods in Computational Mechanics, *Int J Numer Meth Eng*, 101, 143-181.

Ladeveze, P., Moes, N., 1999, Adaptive Control for Finite Element Analysis in Plasticity, *Comput Struct*, 73, 45-60.

Nübel, V., Düster, A., Rank, E., 2007, An *rp*-Adaptive Finite Element Method for the Deformation Theory of Plasticity, *Comput Mech*, 39, 557-574.

Peric, D., Dutko, M., Owen, D., 1998, *Aspects of Adaptive Strategies for Large Deformation Problems at Finite Inelastic Strains*, Advances in Adaptive Computational Methods in Mechanics, eds, Ladeveze, P., Oden, J.T., 349-363, Elsevier.

Peric, D., Hochard, Ch., Dutko, M., Owen, D., 1996, Transfer Operators for Evolving Meshes in Small Strain Elasto-Plasticity, *Comput Method Appl M*, 137, 331-344.

Serafin, M., Cecot, W., 2010, Toward Two-Scale Adaptive FEM Modeling of Nonlinear Heterogeneous Materials, *Int J Multiscale Com*, 8, 303-317.

Schwab, C., 1998, *p- and hp- Finite Element Methods: Theory and Applications in Solid and Fluid Mechanics*, Oxford University Press, New York.

Simo, J. C., Hughes, T. J. R., 1998, *Computational Inelasticity*, Springer-Verlag, New York.

Simo, J. C., Taylor, R. I., 1986, Return Mapping Algorithm for Plane Stress Elastoplasticity, *Int J Numer Meth Eng*, 22, 649-670.

Szabo, B., Düster, A., Rank, E., 2004, *The p-Version of the Finite Element Method*, Encyclopedia of Computational Mechanics, John Wiley & Sons, 1-5.

Wunderlich, W., Cramer, H., Steinl, G., 1998, An Adaptive Finite Element Approach in Associated and Non-Associated Plasticity Considering Localization Phenomena, *Adaptive Computational Methods in Mechanics*, eds, Ladeveze, P., Oden, J.T., 293-332. Elsevier.

Zienkiewicz, O. C., Huang, G. C., Liu, Y. C., 1990, Adaptive FEM computations of forming processes – application to porous and non-porous materials, *Int J Numer Meth Eng*, 30, 1527-1553.

AUTOMATYCZNA *HP*-ADAPTACJA DLA ZAGADNIEŃ SPRĘŻYSTO-PLASTYCZNYCH

Streszczenie

Metoda *hp*-adaptacji jest techniką, która dla zagadnień liniowych gwarantuje szybką, udowodniona teoretycznie, zbieżność eksponencjalną błędu. Wykorzystaliśmy tą metodę dla wybranych problemów sprężysto-plastycznych ze stowarzyszonym prawem płynięcia i powierzchnią plastyczną Misesa. Zaproponowaliśmy modyfikację estymatora błędu sterującego podziałami elementów. Zaobserwowaliśmy zbieżność eksponencjalną, gdy krawędź elementu skończonego pokrywa sie z granicą strefy sprężysto-plastycznej.

Received: November 20, 2014
Received in a revised form: November 25, 2014
Accepted: November 27, 2014